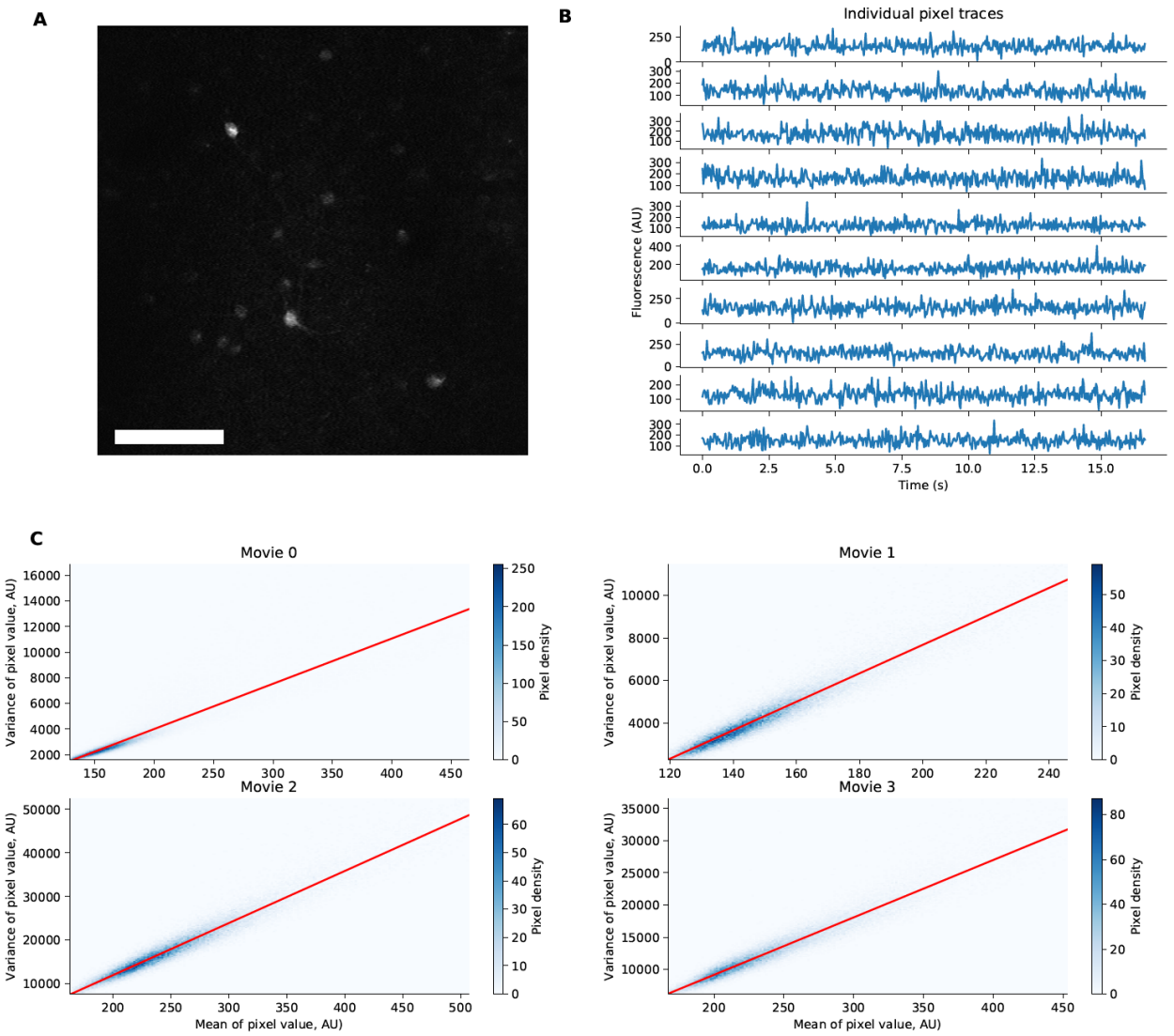

Supplementary Fig. 1 | Poisson or shot-noise dominates single-pixel variance in two-photon microscopy. (A) An example single frame extracted from a two-photon imaging experiment. Scale bar is 100 µm. (**B**) Fluorescence trace from 10 randomly selected pixels in the same movie as (A). (**C**) Variance against mean for all pixels in 4 different two-photon calcium imaging movies collected *in vivo*. The linearity indicates that poisson noise dominates individual pixel variation. The slope of the red line is the amplification gain of the microscope. Scale bar is 100 µm.

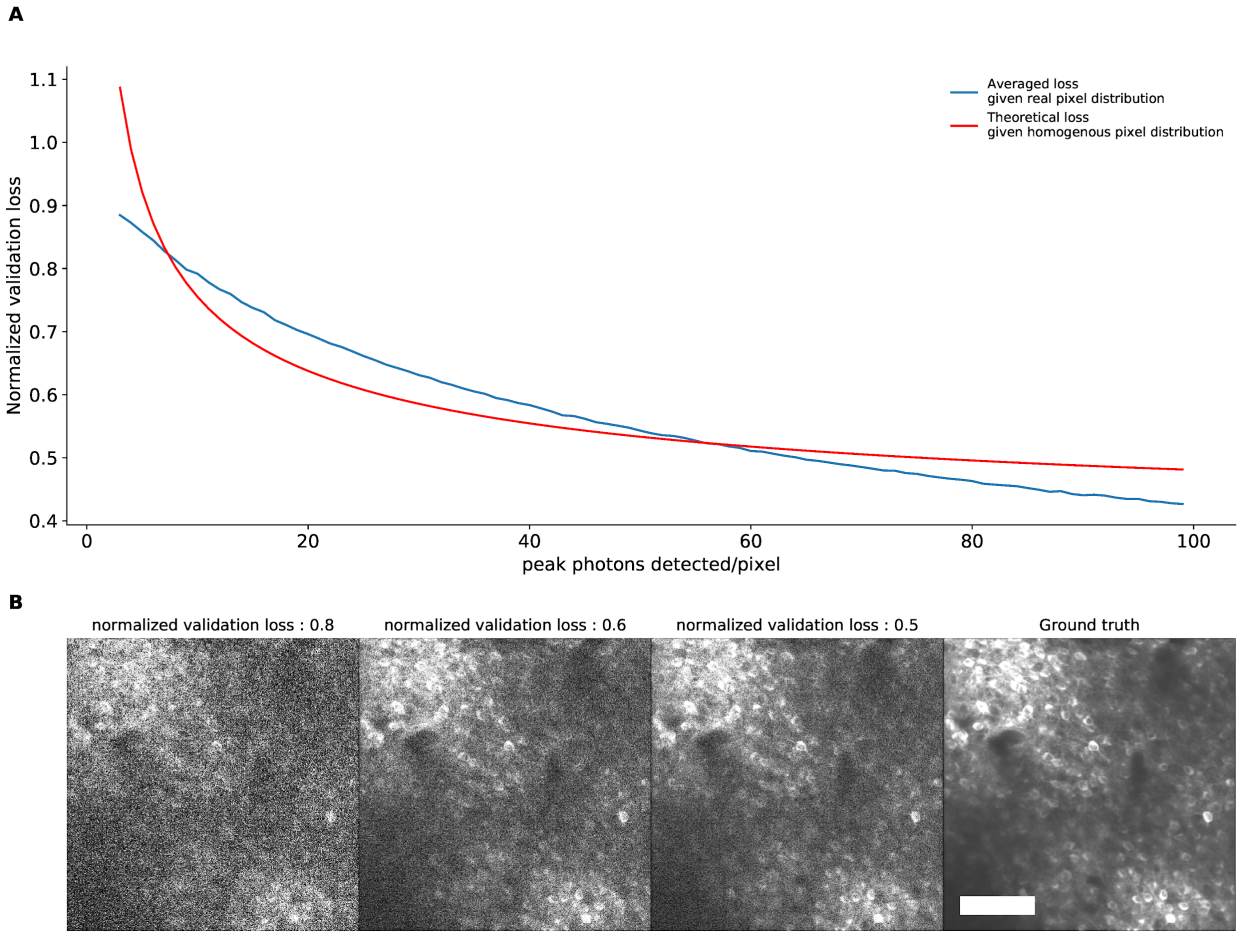

Supplementary Fig. 2 | Simulation of the relationship between mean absolute error and ground truth. **(A)** The normalized mean absolute error was simulated between an averaged two-photon image (Ground truth, see panel B) and various levels of shot noise. Shot noise was modulated by changing the peak number of photons detected in the image per pixel. Red curve was calculated assuming a homogeneous distribution of intensity and a shot noise limited SNR. (**B**) Example individual images associated with a specific normalized validation loss. Scale bar is 100 μm.

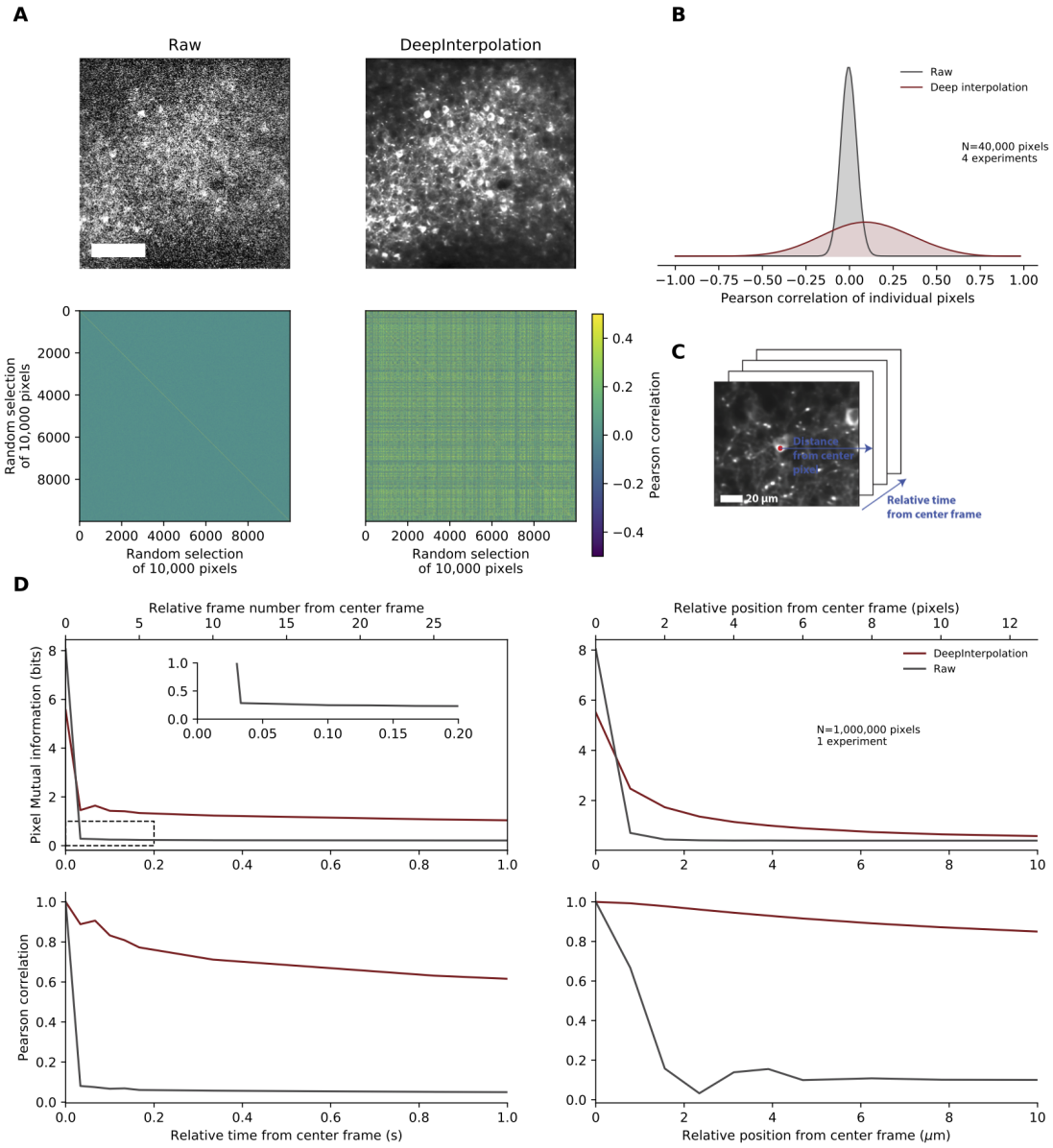

Supplementary Fig. 3 | Correlation and mutual information of pairs of pixels before and after DeepInterpolation. (**A, top row**) Individual frames of a two-photon calcium movie before and after DeepInterpolation. Scale bar is 100 µm. (**A, bottom row**) Pairwise Pearson correlation of a random selection of 10,000 pixels from top movie. **(B)** Distribution of Pearson correlation for 40,000 pixels randomly selected from 4 different experiments (KS test comparing Raw with DeepInterpolation: $p = 9e^{-71}$, $n = 1000$ pixels randomly selected) (**C**) Schematic illustrating the spatial and temporal distances used in (D). (**D, left, top row**) Mutual information between a center pixel and consecutive frames as indicated in schematic (C). The mutual information at the origin is the pixel entropy, illustrating how many bits of information are necessary to encode an individual pixel independently. Inset highlights a small baseline mutual information between consecutive frames in raw data. (**D, left, bottom row**). Same as (**D, top**) but plotting the Pearson correlation. (**D, right, top row**). Mutual information between a center pixel and its neighboring pixel in the same frame along a horizontal axis as shown in (C). (**D, right, bottom row**). Same as (D, top) but plotting the Pearson correlation.

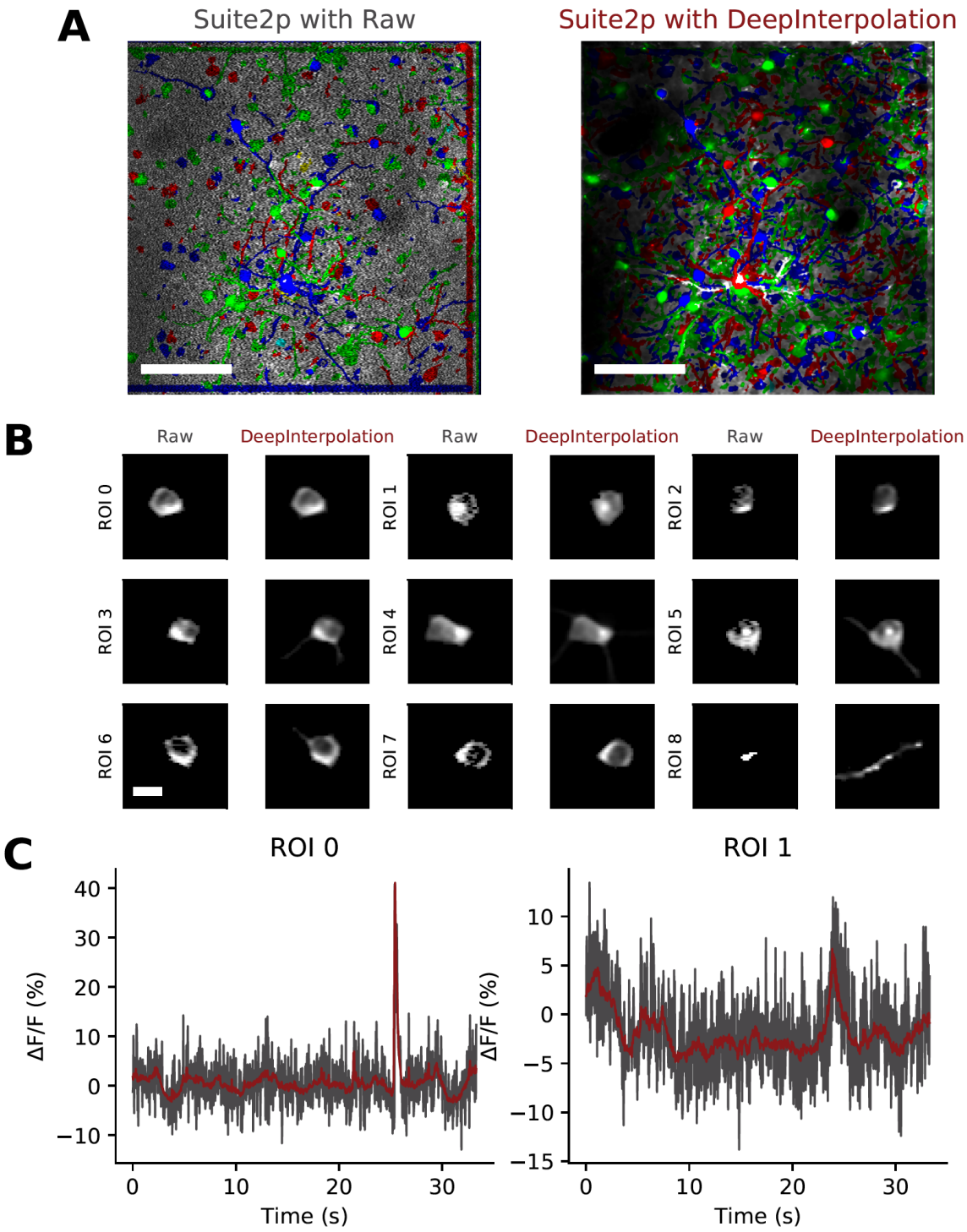

Supplementary Fig. 4 | Cell segmentation with Suite2p with and without DeepInterpolation. (A) Overlay of segmentation filters on top of a single frame of data with (**left**) and without DeepInterpolation (**right**). Scale bar is 100 μm. **(B)** Example cell-matched segmentation filters found by Suite2p with the same segmentation settings (default values) with and without DeepInterpolation. Scale bar is 10 μm. (**C**) 2 examples matched calcium traces after segmentation with Suite2p.

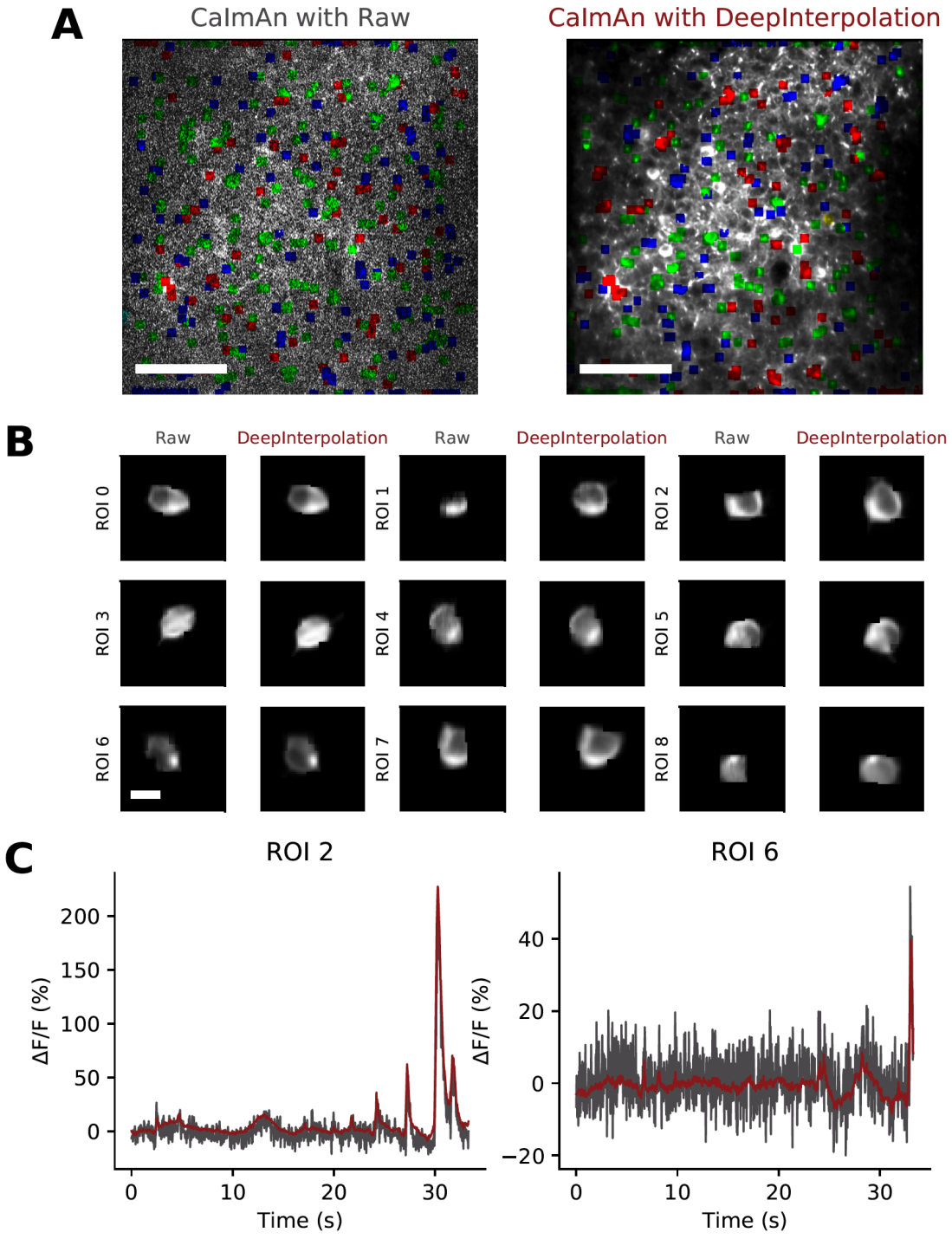

Supplementary Fig. 5 | Cell segmentation with CaImAn with and without DeepInterpolation. (A) Overlay of segmentation filters on top a single frame of data with (**left**) and without DeepInterpolation (**right**). Scale bar is 100 μm. **(B)** Example cell-matched segmentation filters found by CaImAn with the same segmentation settings (default values) with and without DeepInterpolation. Scale bar is 10 μm. (**C**) 2 examples matched calcium traces after segmentation with CaImAn.

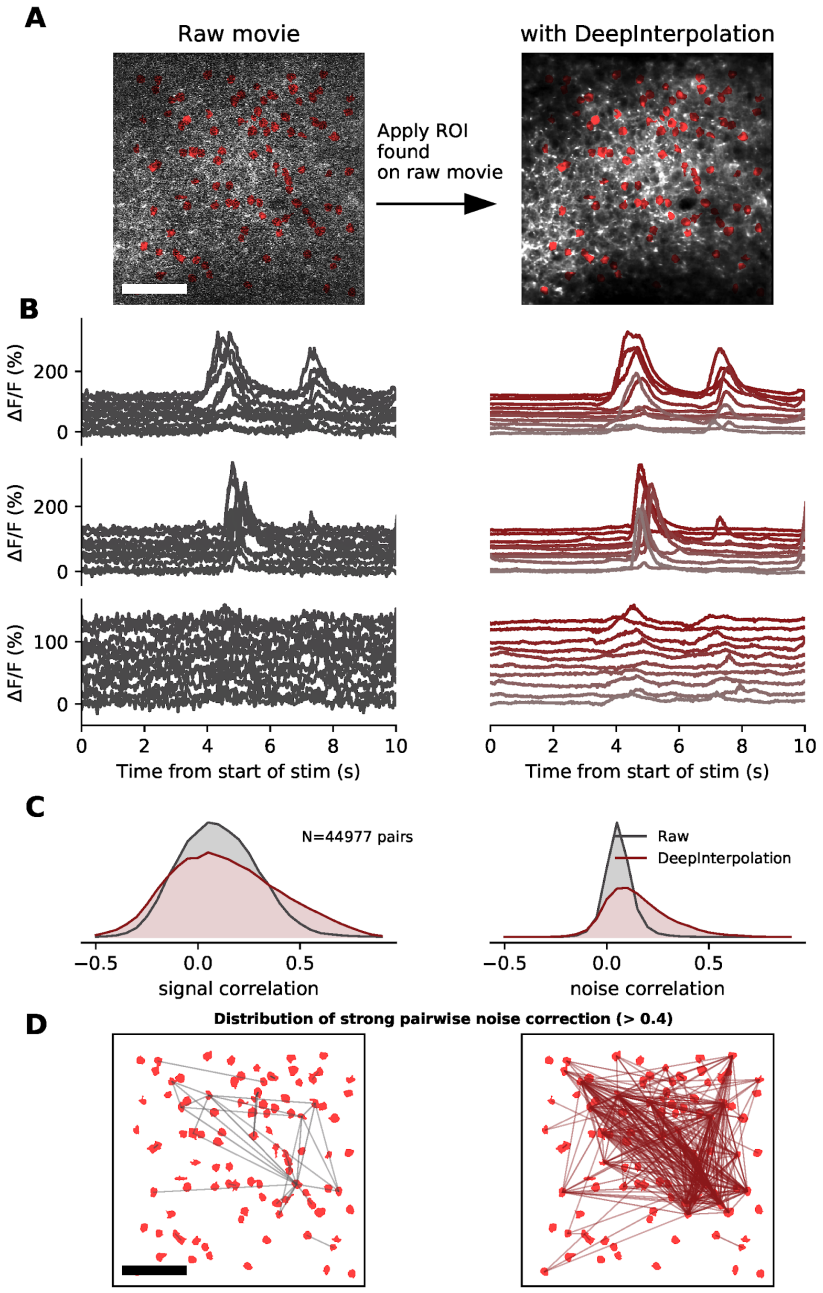

Supplementary Fig. 6 | Applying region-of-interests (ROIs) detected on noisy raw data also showcases increased signal and noise correlation. (A) 99 ROIs detected on the original, non-denoised, movie were overlaid on top of a single frame from the original movie as well as the same frame after DeepInterpolation. These ROI were used to extract traces in (B). Scale bar is 100 µm. (**B**) Example temporal response from 3 neuronal somas to 10 repeats (one trace per repeat) of a natural movie presentation. Left: ROI filter was applied to the original movie. Right: ROI filter was applied to the denoised movie. **(C, left)** signal correlation (average correlation coefficient between the average temporal response of a pair of neurons) for all pairs of ROI in for both raw and denoised traces. **(C, right)** noise correlation (average correlation coefficient at all time points of the mean-subtracted temporal response of a pair of neurons) for all pairs of ROI in **(A).** Distributions were created from 4 separate experiments with a total of 44,977 pairs of neurons. (**D**) Pairs of neuronal somas with high noise correlation (>0.4) are connected with a straight line for the original two-photon data (37 pairs on the left) and after DeepInterpolation (329 pairs on the right).

Supplementary Note | DeepInterpolation pseudocode for denoising two-photon Ca^{2+} imaging.

1. **Training**
    a. Generate a randomized list of $N_{training}$ frames from P separate two photon movies.
    b. Calculate a single pair of sample mean and pixel standard deviation for each movie using all pixels in the first 100 frames.
    c. Store randomized list of frame index, movie data storage location and associated sample mean and standard deviation in a json file.
    d. Repeat a,b, c for validation test data on a separate set of N_{test} movies.
    e. Load json file associated with training samples and test samples.
    f. Load json file with training meta-parameters.
    g. Initialize training data generators for both training and testing data. Generator is pulled from a local library of generators based on training meta-data. Training generator is directly streamed from a network disk location during training by multi-threaded workers. Validation generator is pre-loaded in memory for caching.
    h. Initialize training network architecture. Architecture is pulled from a local python library based on a single string descriptor.
    i. Initialize training callbacks to save and monitor model progression throughout training.
    j. Initialize loss to "mean_absolute_error".
    k. Initialize optimizer to RMSProp.
    l. Compile model for training.
    m. Start training loop on local GPUs
        i. For each batch of training, load 5 samples from the randomized list. Both input and output samples are z-scored using pre-computed mean and standard deviation (see **b**)
        ii. Monitor training and validation loss throughout training.
        iii. Save trained model every 12500 samples.
        iv. Interrupt training based on validation training convergence.
2. **Inference**
    a. Select one movie for inference
    b. Calculate mean and standard deviation of 100 frames initial segment
    c. Load trained DeepInterpolation model
    d. For each frame in the movie (excluding N_{pre} and N_{post} frames respectively at the onset and end of the movie):
        i. Z-score N_{pre} and N_{post} frames respectively before and after the selected frames, using pre-computed mean and standard deviation.
        ii. Predict the output frame using the DeepInterpolation model
        iii. Convert output frame back to original pixel values using precomputed mean and standard deviation.

Experiment ID	Probe ID	Start time	Brain Structures	Used for training
778998620	792626851	4665.8179 s	VISl (LM), CA1, CA3	No
787025148	792586842	4672.1967 s	VISp (V1), SUB, LP	No
768515987	773549856	4672.2224 s	VISrl (RL), CA1, DG, APN	Yes
794812542	810758787	4665.8332 s	VISrl (RL), CA1, DG, APN	No
778998620	792626853	4665.8179 s	VISal (AL), CA1, CA3, DG, LGv	No
767871931	773462997	4672.2352 s	VISal (AL), CA1, CA3, DG, LT	Yes
779839471	792645501	4672.3841 s	VIS, CA1, CA3, DG, LGd	No
771160300	773621948	4672.3791 s	VISal (AL), CA1, CA3, DG, LGd	Yes
781842082	792586881	4672.1312 s	VISp (V1), SUB, SGN	No
793224716	805124815	4675.2401 s	VISrl (RL), CA1, DG, LP, APN	No

Supplementary Table 1. Details of Neuropixels data used for DeepInterpolation training and inference.

References

1. Krull, A., Buchholz, T.-O. & Jug, F. Noise2void-learning denoising from single noisy images. in *Proceedings of the IEEE Conference on Computer Vision and Pattern Recognition* 2129–2137 (2019).
2. Buchanan, E. K. *et al.* Penalized matrix decomposition for denoising, compression, and improved demixing of functional imaging data. doi:10.1101/334706.
3. Charles, A. S., Song, A., Gauthier, J. L., Pillow, J. W. & Tank, D. W. Neural Anatomy and Optical Microscopy (NAOMi) Simulation for evaluating calcium imaging methods. doi:10.1101/726174.
4. Huang, L. *et al.* Relationship between simultaneously recorded spiking activity and fluorescence signal in GCaMP6 transgenic mice. *Elife* **10**, (2021).
5. Friedrich, J., Zhou, P. & Paninski, L. Fast online deconvolution of calcium imaging data. *PLoS Comput. Biol.* **13**, e1005423 (2017).